

## Application of Modified PANI-ZnO Composites for NH<sub>3</sub> Gas Sensor at Ambient Temperature

<sup>1</sup>Naimat Ullah\*, <sup>2</sup>Anwar -Ul-Haq Ali Shah, <sup>3</sup>Fazal Akbar Jan, <sup>1</sup>Rotaba Ansir, <sup>4</sup>Wali Muhammad

<sup>1</sup>Department of Chemistry, Quaid-i-Azam University, Islamabad, Pakistan.

<sup>2</sup>Institute of Chemical Sciences University of Peshawar, Khyber-Pakhtunkhwa, Pakistan

<sup>3</sup>Department of Chemistry Bacha Khan University Chrasadda, Khyber-Pakhtunkhwa, Pakistan

<sup>4</sup>Department of Biotechnology, Quaid-i-Azam University, Islamabad, Pakistan.

[naimatullah@chem.qau.edu.pk](mailto:naimatullah@chem.qau.edu.pk)\*

(Received on 3<sup>rd</sup> July 2019, accepted in revised form 21<sup>st</sup> October 2019)

**Summary:** Polyaniline and zinc oxide nanoparticles were successfully synthesized through inverse emulsion polymerization method and hydrothermal method respectively. For ammonia gas sensing using LCR meter thin film of the composite was fabricated by using spin coater. The functional groups, morphological, optical, structural properties of zinc oxide nanoparticles, polyaniline (emeraldine salt) and composites were investigated by FTIR spectroscopy, Scanning electron microscopy (SEM), UV-Visible spectroscopy and XRD analysis. The formation of ZnO particles of different shapes in the nano range was confirmed from UV-visible and XRD analysis. UV visible spectrum shows the formation of nanoparticles of ZnO. Thin film of Polyaniline/zinc oxide composites were deposited on the surface of copper interdigitated electrode. The fabricated device showed sensitivity to ammonia gas (NH<sub>3</sub>) at ambient temperature (300 K). It was observed that the resistance is decreases with the increase of volume of ammonia gas. The electrical properties were also investigated of the different concentration of nanocomposite. Optimum sensing response was achieved with PANI in the presence of 50 wt% ZnO nanoparticles. It may also be inferred from this study that the solution mixing process to produce composites has promising future if handled carefully.

### Introduction

Recently, Interest has been given to acquire brand new materials for the sensing applications. Gas sensor is playing a vital role throughout our environment keeping track of home protection as well as chemical preventing [1]. Nowadays, several emergent purposes employ organic components intended for knowing inexpensive equipment, ranging from chemical substance and gas sensors, to organic technology, also to the growth involving low-priced photovoltaic cells and field-effect transistors. The units frequently work with innovative components which include conjugated polymers and nanostructure inks, compatible with inexpensive depositing equipment [2]. Various parameters which are responsible for the better performance of metal oxide sensors, conducting polymers and ionic conductors are structure, operating temperature and morphology [3]. In this regard, many products like metal oxides, sensitive organic layers, conducting polymers [4], CNTS based sensors [5] both, individually and on cellulose paper [6] or cotton textile [7] have been used as sensors. All the materials have been substantially synthesized for the efficient, reliable and stable gas sensing applications. Over the past few decades, various researchers have explored and reported about the metal oxide gas sensors [8]. Lately conducting polymers have also been employed as a gas sensor due to primary merits for instance effortless functionality along with area temperatures operation [1]. Conducting polymers are very important and

exciting type connected with organic conductors. Polyaniline is an attractive candidate among all other members of this family due to simplicity of preparation, large setting stability, secure electrical conduction device as well as special properties [9]. Polyaniline promises to have fascinating attributes as resources intended for standard rechargeable batteries, modified electrodes, electro chromic exhibit products, and gas sensors [10]. However, the down sides with these executing polymers are generally their own minimal running power, poor chemical stability and also hardware durability [1]. The issue with these conducting polymers has been there lower process ability in addition to poor mechanical strength in addition to poor chemical stability. It is essential to plan a simple method to fabricate a thin film to plan an effective sensor [11].

It's been documented that organic-inorganic hybrid material can certainly synergize as well as enhance the properties of pure organic or inorganic materials throughout electronics, optics, coating, catalysis and so on. Various composites regarding PANI with inorganic material; in addition to polymeric counterparts have been synthesized in addition to useful for improving the actual sensor sensitivity lately. For instance, a nanocomposite of PANI/TiO<sub>2</sub> can detect the ammonia gas concentration up to ~20

---

\*To whom all correspondence should be addressed.

ppm but when Ag modified PANI is used it can detect 5ppm of ammonia gas etc[12].

Recently, wide band gap semiconductors based sensors have also been developed. One of these materials is n type ZnO based sensors. So keeping in view the efficiency of ZnO nanoparticles based sensors an effort has been made to develop a nanocomposite of ZnO nanoparticles [13] and p-type conducting polymer Polyaniline (PANI), which leads to PN heterojunction in which the p-type PANI, a p type conductive material, tend to stick around the exterior of electro-spun semi-conductive ZnO nanoparticles [12]. Recently, we have tried to use PANI and ZnO nanoparticles to observe the NH<sub>3</sub> gas sensing at ambient temperature (300K).

By using this nanocomposite, a study has been conducted to develop custom build Ammonia (NH<sub>3</sub>) gas sensing setup and to study the ammonia gas sensing variation according to temperature unity variation around room temperature. The actual PANI/ZnO composites were characterized by use of XRD, FTIR, SEM and UV- Visible spectroscopy.

## Experimental

### Chemicals

Zinc nitrate (BDH laboratory suppliers), Aniline (Acros) was distilled and stored under nitrogen, while Chloroform (Scharlau), Benzoyl Peroxide (Merck), 2-Butanol (Aldrich), DBSA (Acros), Toluene (Scharlau), Acetone (Qualigens), N-methyl-2-pyrrolidone (Qualigens), Sodium hydroxide (Merck) were used as received.

### Synthesis of polyaniline salt

Polyaniline salt was synthesized through inverse emulsion polymerization. For this purpose, a round bottom flask was taken and 0.29 mol of chloroform was placed in it. Under constant stirring, 1.25 mmol of benzoyl peroxide was added into the solvent. 2-butanol, DBSA and aniline were added into resultant mixture at optimized concentration. After that, 0.28 mol of deionized water was added which resulted in the formation of milky solution. The mixture was let to stir for 5h which ultimately turned it green, and then reaction was proceeded for another 24h period. At the end, the organic phase having the polyaniline salt was separated and washed several times using acetone and deionized water.

### Synthesis of ZnO nanoparticles

The zinc oxide (ZnO) nanoparticles were prepared by hydrothermal method shown in Fig. 1. At start, 0.473 g of zinc precursors (Zn (CH<sub>3</sub>COO)<sub>2</sub>·6H<sub>2</sub>O)) was taken in 25 ml of ethanol. 0.1 M NaOH was added to obtain the optimum pH 8-10. The solution was stirred for ten minutes to obtain a homogeneous solution. The resultant mixture was transferred in an autoclave and kept at 200 °C for 6 hours. The precipitated solution was washed several times with water and ethanol to get the product. The final product was obtained after drying at 50 °C.

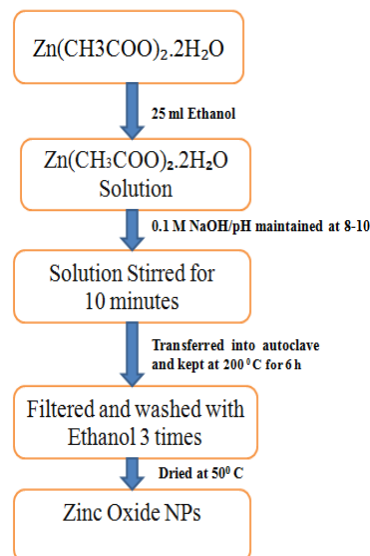


Fig. 1: Schematic representation ZnO NPs synthesis.

### Synthesis of PANI/ZnO nanocomposite

To synthesize the PANI/ZnO nanocomposite solution processed route was adopted. 4% solution of Polyaniline powder and zinc oxide nanoparticles are prepared in N-methyl-2-pyrrolidone. The solution was allowed to stir for 5h. Different composition of Polyaniline powder and zinc oxide nanoparticles were prepared, 60 %PANI with addition of 40% ZnO nanoparticles, 50% PANI with addition 50% ZnO nanoparticles, 30 %PANI with addition 70 % ZnO nanoparticles.

### Coating of the composite on interdigitated electrode

Different composition of Polyaniline powder and zinc oxide nanoparticles composites which is already mention in above table were coated on interdigitated electrode with 1500 rpm through spin coating technique shown in Fig.:2.

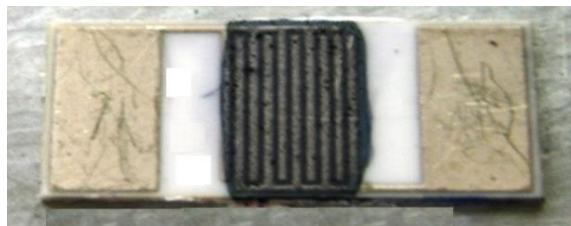


Fig. 2: Composite coated interdigitated electrode.

## Results and Discussions

### FTIR spectroscopic study

Fig 3a depicts the spectrum of pure PANI. The bands at  $3718\text{ cm}^{-1}$  illustrate the existence of OH group of the water which is added as a dispersion medium during the polymerization. While the peak at  $2950\text{ cm}^{-1}$  shows the symmetric and asymmetric stretching vibration of C-H bonds of DBSA [14]. The band at  $2351\text{ cm}^{-1}$  predicts the unsaturated amine (N-H) group in the stretching mode [15]. The bands present at  $1548\text{ cm}^{-1}$  and  $1483\text{ cm}^{-1}$  are arisen due to the quinod and benzoid group of the aromatic rings which give rise to stretching vibration of C=C [16]. The secondary aromatic amine group was predicted by the C-N stretching vibration of aromatic ring at  $1310\text{ cm}^{-1}$  [17]. A band at  $1220\text{ cm}^{-1}$  is owing to the stretching vibration of  $\text{SO}_4$  anions in DBSA [18]. The peak at  $1120\text{ cm}^{-1}$  specifies the amine and imine functional group. The para substitution of 1, 2, 4 aromatic ring is attributed to the rise of a band at  $875\text{ cm}^{-1}$ . The peak around  $670\text{ cm}^{-1}$  depicts the presence of sulfonate group in the DBSA present in PANI [19]. The peak at  $577\text{ cm}^{-1}$  identifies the C-H bending vibration out of the plane [20]. The observed IR-bands verify a successful synthesis of PANI. FTIR spectrum of the synthesized ZnO nanoparticles showed (Fig.3b) the fundamental mode of vibration at  $3450.887\text{ cm}^{-1}$  which correspond to the O-H stretching vibration [21]. The peaks around  $2936\text{ cm}^{-1}$  and  $1391\text{ cm}^{-1}$  are due to the C-H stretching and asymmetric C=O stretching vibration. While C=O symmetric stretch give rise to a band around  $1648\text{ cm}^{-1}$ . The peak at  $857\text{ cm}^{-1}$  is a result of the tetrahedral coordination of Zn. While O-H bending gives a peak at  $556\text{ cm}^{-1}$ . The absorption at  $1126\text{ cm}^{-1}$  is a proof of saccharide structure while at  $1028\text{ cm}^{-1}$  C-O stretching vibration band is observed. C-O bond stretch gives a peak at  $752\text{ cm}^{-1}$ . ZnO nanoparticles showed a stretching vibration at  $648.85\text{ cm}^{-1}$  [22]. FTIR spectrum of the synthesized PANI/ZnO nanoparticles composite showed (Fig. 3c). The spectrum at  $1308\text{ cm}^{-1}$  is for C-N stretching vibrations, [23] the spectrum at  $1139.93\text{ cm}^{-1}$  and  $1674\text{ cm}^{-1}$  is for N=Q=N and C=N of iminoquinone stretching respectively [24]. When PANI/ZnO composite was subjected to FTIR, the

absence of any extra peak was observed. Although a minor shift was observed which confirmed the interaction between ZnO and molecular chain of PANI. There is a possibility of hydrogen bonding between ZnO and the NH group of PANI which can be a reason of this shift [25]. C-H bending of aromatic ring gives us  $655\text{ cm}^{-1}$  peak and  $1504\text{ cm}^{-1}$  due to the C-N stretching of benzoid ring. Moreover, a peak appeared at  $3477\text{ cm}^{-1}$  which could be arisen due to the interaction of ZnO NPs with PANI by forming H-bonds between NH and ZnO, so this could be an explanation for the displacement of peak that was observed in spectrum [26]. In  $3300\text{--}3500\text{ cm}^{-1}$  a decrease in intensity was observed which could be due to the fact that Zn is a transition metal, so it can form a coordination complex with N-atom of PANI. The nanocomposite gives a peak at  $2942\text{ cm}^{-1}$  [27]. These interactions can lead to the weakening of N-H in PANI macromolecules. All these results lead to the conformation of the presence of ZnO in composite [28].

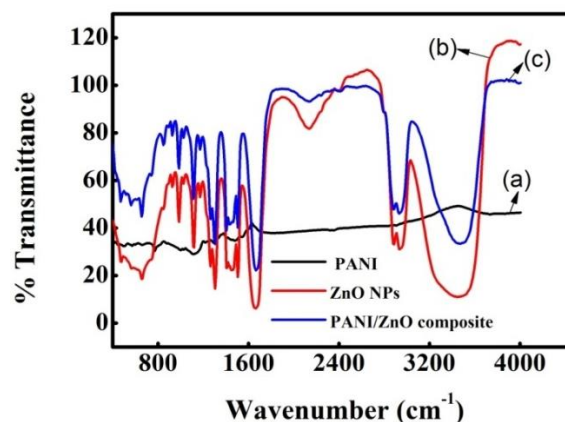


Fig. 3: FTIR Spectra of (a) PANI, (b) ZnO NPs and (c) PANI/ZnO composite.

### Scanning Electron Microscopic Study

The SEM micrograph of pure PANI is described in Fig 4B which shows irregular and high agglomerated pellet like polycrystalline morphology [29]. This is because of unsystematic association of phenazine nucleates and its rapid conversion to start the growth of polymer before the symmetric organization of nucleates throughout polymerization. The morphology can also be affected by greater number of entangle molecules while polymer aggregation, as a result this affect may also contribute to impart pellet like morphology to PANI [30]. In Fig 4A is SEM picture for the ZnO nanoparticles. The Fig shows obviously that the nanoparticles are homogeneous and granular size. Fig 4c depicts the SEM images of 40% ZnO nanoparticles modified PANI composite. The absence of any agglomeration

was confirmed in SEM images of nanocomposite of ZnO/PANI and there is a uniform distribution of the ZnO particles in the PANI matrix [28]. Polyaniline and addition of zinc oxide 50%, and 70% nanoparticles are shown in the Fig 4D, and 4E respectively. It is clearly seen in the Fig 4C that ZnO nanoparticles are

suspended in the composite with Polyaniline. However, the granular surface morphology was changed to smooth as the concentration of the ZnO was increased as shown in the Fig 4D and 4E. These results accomplished in the present study are a good choice of the composite to use in the  $\text{NH}_3$  gas sensor.

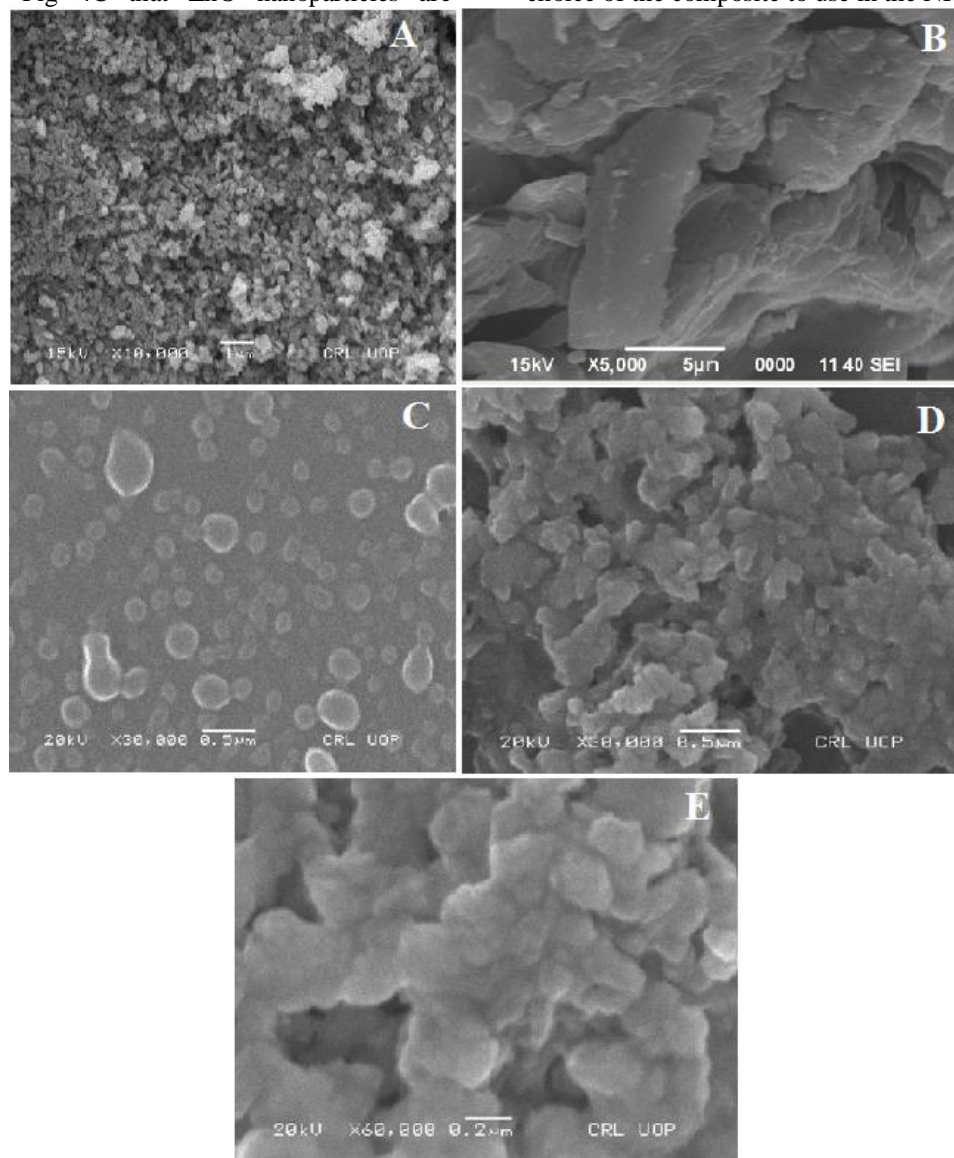


Fig. 4: SEM images of ( A) pure ZnO NPs, (B) pure PANI,(C) 40% ZnO addition,(D) 50% ZnO addition, (E) 70% ZnO addition.

#### UV- Visible spectroscopic Study

The optical study of ZnO NPs was carried out in ethanol as a solvent and the materials were dispersed (Fig 5e). ZnO nanoparticles showed a peak at 365 nm. The UV/visible spectrum corresponding to pure PANI samples dispersed in N-methyl-2-pyrrolidone (NMP) are shown in Fig 5d. Two

absorption peaks at 330 nm and 634 nm are observed which are the characteristic peaks of PANI. These absorption bands in UV region are the result of  $\pi-\pi^*$  transitions of aromatic nuclei and peaks in the region of visible are due to the interaction between benzene nuclei and quinone di-imine structure. No peak of pure ZnO nanoparticles was observed in pure PANI sample

[8]. Fig 5a, 5b, 5c is the UV-visible spectra of different percentage of PANI and ZnO nanocomposites.

Composite of 40% ZnO nanoparticles, 50% ZnO nanoparticles and 70% ZnO nanoparticles has an absorption peaks at 317 nm, 315 nm and 303 nm, respectively. An apparent shift was observed in case of PANI (330 nm) and ZnO (365 nm). The explanation of this shift lies in the interaction between PANI and ZnO which results in a facile exchange of electron from PANI to ZnO via H-bonding [31].

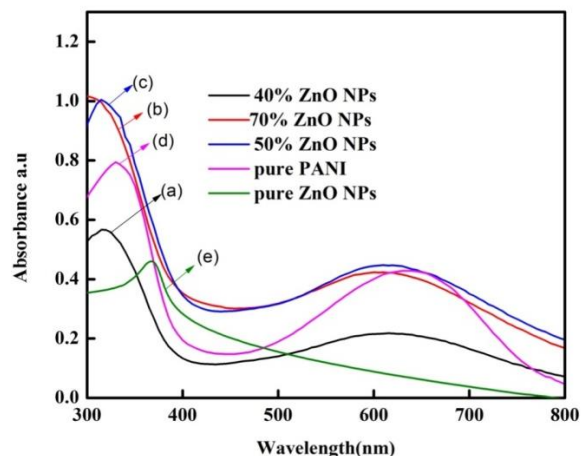
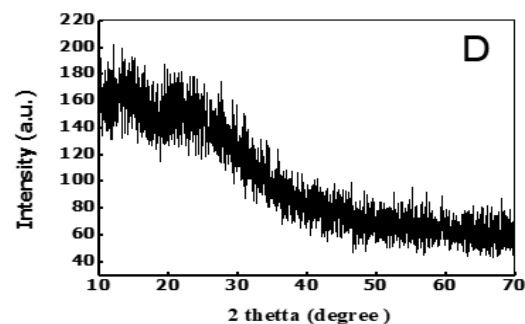
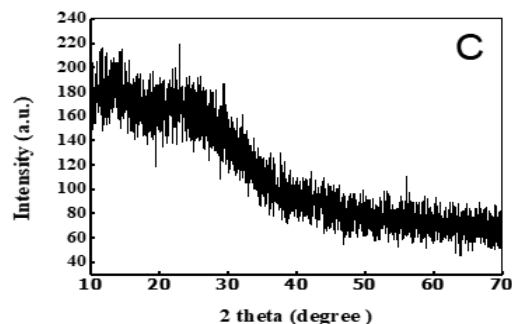
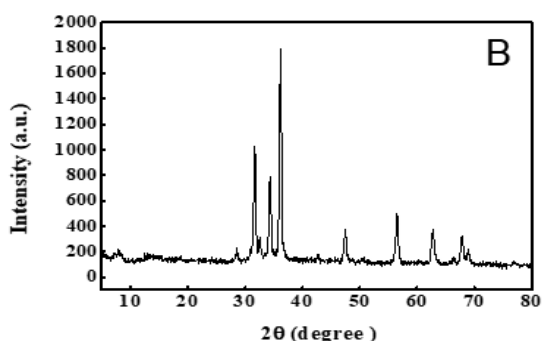
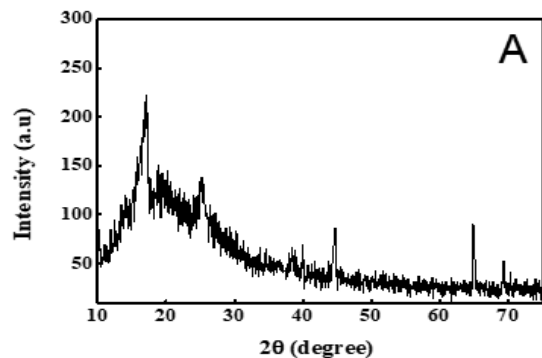


Fig.. 5: UV-Vis spectra of (e) pure ZnO NPs, (d) pure PANI, (a) 40% ZnO addition, (c) 50% ZnO addition, (b) 70% ZnO addition.

#### X-ray diffraction Study

Fig 6A shows the XRD pattern of PANI which is in closed resemblance with previously reported literature. The respective spectrum represents a wide elevated angle asymmetric peak scattering  $2\theta$  stuck between 15- 25°, which indicate the lesser amorphous nature of PANI. The obtained peaks cover one broad peak located around 25.28 ° equivalents to d-spacing of 3.5256 Å, specify a small level of crystallinity [32]. Fig 6b shows the xrd results for selected samples and for pure ZnO NPs the peaks are observed at ( $2\theta = 31.8340, 34.4853, 36.3303$  and  $47.6017$  and  $2\theta = 56.6575$ ). The highest picks were coming out at same angle 36.50. So the peaks shows that the ZnO NPs is crystalline structure [33]. In Fig 6C, 6D and 6E were the XRD pattern of PANI/ ZnO composites, no significant change was observed in peak pattern. But the results suggested that PANI could cause a distortion in ZnO crystal structure upto a certain extent. The results also showed that polyaniline possessed an amorphous structure. This helps understanding the effect that polyaniline incorporation cause the structure of ZnO to get distorted but does not destroy the crystal structure completely. The

amorphous nature of PANI has also been confirmed. A small change in the amorphous behavior of the synthesized composites was responsible for altering the crystalline nature.



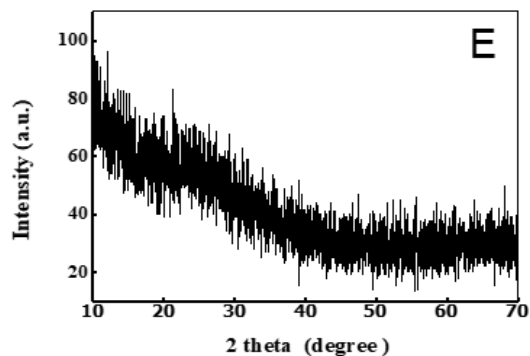


Fig. 6: X-ray diffraction pattern of (A) pure PANI, (B) pure ZnO NPs, (C) 40% ZnO addition, (D) 50% ZnO addition, (E) 70% ZnO addition.

#### *NH<sub>3</sub> gas sensing property of PANI/ZnO composite*

The NH<sub>3</sub> gas sensing property of PANI/ZnO composite films were analyzed simply by using a custom build Ammonia gas Sensing setup shown in Fig 7. In order to evaluate the actual gas response, the actual level of resistance in the PANI/ZnO composite films were measured through LCR meter at ambient temperature and also in NH<sub>3</sub> gas atmosphere. Actual gas response in the form of resistance, a couple of copper electrodes, divided by 1 cm, have been put on PANI/ZnO films coated interdigitated electrode and silver wires were attached to the connectors (terminals) of LCR meter. For monitoring the response of the composite film NH<sub>3</sub> gas was injected through pipe from ammonia gas cylinder. The ammonia gas was diluted in the presence of air and water vapors as the ammonia gas was coming from NH<sub>4</sub>OH solution of 30-33%. The resistance was measured by use of GWINSTEK LCR-817 model LCR meter.

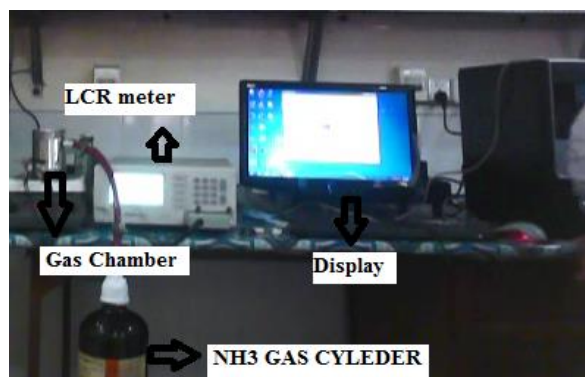


Fig. 7: Image of custom build Ammonia gas Sensing setup.

#### *Sensor components and sensing mechanism*

Fig 8 shows the Image of custom build Ammonia gas Sensing setup, which consist of LCR meter, Ammonia gas cylinder, gas chamber and computer (Display). The ammonia sensing properties of PANI/ZnO composite was observed by using a of custom build Ammonia gas Sensing unit, the gas chamber contain a couple of copper electrodes have been put on interdigitated electrode which fixed in chamber. Copper electrodes wires were attached to the jacks/connectors (terminals) of LCR meter. The large surface area as well as the smaller diameters of polyaniline offers a quick reply time simply because diffusion into a cylinder of smaller diameter is rather quick. All these observations were carried out at room temperature (27°C). The results showed that the sensor response was increased on addition of ZnO to PANI upto a certain limit. After that limit, the increased concentration of ZnO resulted in a decreased activity. Another factor which is responsible for decreased sensitivity of sensor is dependent upon the morphology [8].



Fig. 8: Component of custom build Ammonia gas Sensing setup.

#### *Ammonia gas sensing*

The behavior of sensor prepared by ZnO/PANI was much effective in comparison to the sensor prepared by PANI alone, reported recently [34-36]. The variation of ammonia gas sensing with increasing concentration of the gas is depicted in Fig 9 a, b, c. The response of sensor was observed to be effective with the increase in gas concentration. The addition of ZnO NPs leads to a decrease in resistance of PANI, when the ammonia gas comes in contact with sensing composite of PANI/ZnO composite, because ammonia gas is a reducing gas and donate electrons to the PANI/ZnO composite. When the resistance increases the capacitance will be decreased and vice versa. To characterize a sensor, resistance is an important factor. When the gas is turned on, (Fig.7) PANI/ZnO NPs composite sensor response through varying the resistance of the composite with time. It reveals that the resistance decreases after some interval of time as concentration of NH<sub>3</sub> increased. A possible reason of this decrease is the sufficient no of molecules present at the surface which helps the

reaction to occur. Resistance of 50% ZnO composite is decreased constantly with interval of time due to ZnO NPs granular morphology, the ZnO NPs are equally distributed in PANI and provides a high surface area for the reaction of ammonia sensing and leading to an elevated response. The capacitance shown in Fig 10 change just like the resistance but the main thing is that the resistance decreases and capacitance increases when the interaction occurs between the composite and ammonia gas.

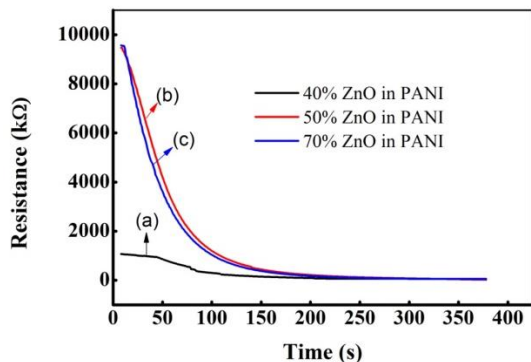


Fig. 9: Resistance vs. time graph of (a) 40% ZnO addition, (b) 50% ZnO addition, (c) 70% ZnO addition.

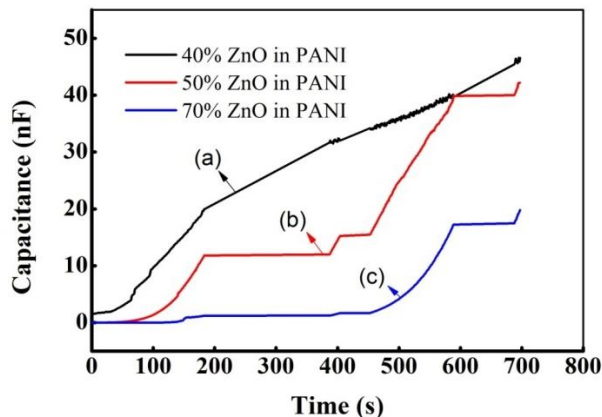


Fig. 10: Capacitance vs. time graph of (a) 40% ZnO addition, (b) 50% ZnO addition, (c) 70% ZnO addition.

The sensing response of the materials was studied by using ammonia concentration at ambient temperature. The concentration of ammonia was varied from 35 to 175 ppm with an addition of 35 ppm every time. The sensitivity of all three composite was recorded towards the ammonia gas and optimized results are compared in Fig 11. There was a rapid increase in response over the exposure of ammonia but after a certain limit the response was quite inclined due to saturation. The increase in sensing at first was due

to the ore molecule adsorb but after a certain limit due to excess amount of molecules the surface become less available and hence the response wasn't more efficient.

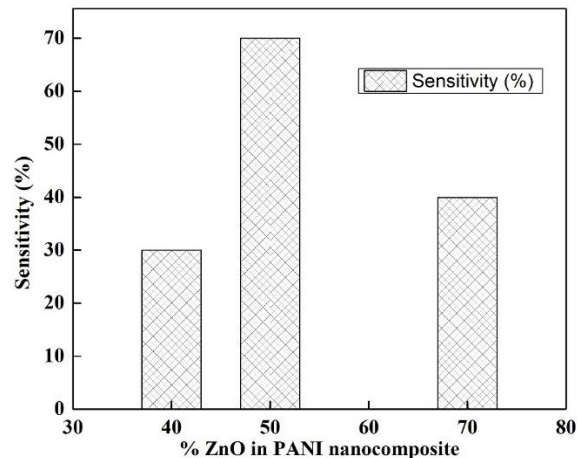


Fig. 11: Effect of %ZnO coupled with PANI on ammonia sensing.

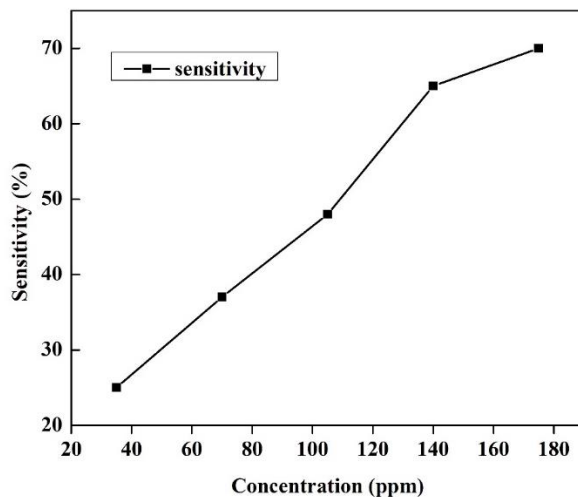


Fig. 12: Effect of ammonia concentration on 50% ZnO nanocomposite with PANI.

Among all nanocomposites, 50% ZnO with PANI showed a highest response towards ammonia sensing with 70% sensitivity as depicted in Fig 12. When ZnO % was increased further, the agglomeration of nanoparticles was observed. This leads to the inclined in sensitivity of sensors with 70%ZnO with PANI.

**Conclusions**

Polyaniline (PANI salt) zinc oxide nanoparticles were prepared by very simple methods. The influence of varying different conditions leads to achieve desired products in both the cases. The separation of ZnO at an early stage of their synthesis is not difficult to handle, while, the handling of PANI synthesis by inverse emulsion polymerization is a little tricky. To prepare the nanocomposite of PANI/ZnO the concentration of ZnO was varied and used as a template to synthesize the nanocomposite with different composition. The nanocomposite of PANI/ZnO was studied by using FTIR. The SEM and XRD results confirmed the uniformity of the samples in the nanocomposite. The ammonia sensing of the composite indicated that newly synthesized composite of PANI/ZnO is an excellent candidate for NH<sub>3</sub> detection. Best results at 50% ZnO modified PANI were obtained at room temperature towards NH<sub>3</sub> gas sensing. The results, obtained through LCR meter, of a sensor prepared by the PANI-ZnO composite showed good selectivity towards ammonia gas.

#### Acknowledgment

This study has not funded by any sources.

#### Conflict of Interest

No conflict of interest was found among the authors.

#### References

1. S. Patil, M. Chougule, S. Sen, and V. Patil, Measurements on room temperature gas sensing properties of CSA doped polyaniline-ZnO nanocomposites, *Measurement*, **45**, 243(2012).
2. A. Arena, N. Donato, G. Saitta, A. Bonavita, G. Rizzo, and G. Neri, Flexible ethanol sensors on glossy paper substrates operating at room temperature," *Sensor Actuat B-Chem.*, **145**, 488 (2010).
3. Q. Fang, D. Chetwynd, J. Covington, C.-S. Toh, and J. Gardner, Micro-gas-sensor with conducting polymers, *Sensor Actuat B-Chem.*, **84**, 66 (2002).
4. S. H. Yu, J. Cho, K. M. Sim, J. U. Ha, and D. S. Chung, Morphology-driven high-performance polymer transistor-based ammonia gas sensor, *ACS Appl. Mater. Interfaces*, **8**, 6570(2016).
5. M. Meyyappan, Carbon Nanotube-Based Chemical Sensors, *Small*, **12**, 2118( 2016).
6. J.-W. Han, B. Kim, J. Li, and M. Meyyappan, A carbon nanotube based ammonia sensor on cellulose paper, *Rsc Advances*, **4**, 549(2014).
7. J.-W. Han, B. Kim, J. Li, and M. Meyyappan, A carbon nanotube based ammonia sensor on cotton textile, *Appl. Phys. Lett.*, **102**, 193104 (2013).
8. V. Talwar, O. Singh, and R. C. Singh, ZnO assisted polyaniline nanofibers and its application as ammonia gas sensor, *Sensor Actuat B-Chem.*, **191**, 276 (2014).
9. D. Xie, Y. Jiang, W. Pan, D. Li, Z. Wu, and Y. Li, Fabrication and characterization of polyaniline-based gas sensor by ultra-thin film technology, *Sensor Actuat B-Chem.*, **81**, 158 (2002).
10. Q. Pei and X. Bi, Electrochemical preparation of electrically conducting polyurethane/polyaniline composite, *J. Appl. Polym. Sci.*, **38**, 1819 (1989).
11. M. Matsuguchi, A. Okamoto, and Y. Sakai, Effect of humidity on NH<sub>3</sub> gas sensitivity of polyaniline blend films, *Sensor Actuat B-Chem.*, **94**, 46 (2003).
12. J. Gong, Y. Li, Z. Hu, Z. Zhou, and Y. Deng, Ultrasensitive NH<sub>3</sub> gas sensor from polyaniline nanograin enched TiO<sub>2</sub> fibers, *J. Phys. Chem. C*, **114**, 9970 (2010).
13. E. Traversa, M. Miyayama, and H. Yanagida, Gas sensitivity of ZnO/La<sub>2</sub>CuO<sub>4</sub> heterocontacts," *Sensor Actuat B-Chem.*, **17**, 257(1994).
14. S. V. Kasisomayajula, X. Qi, C. Vetter, K. Croes, D. Pavlacky, and V. J. Gelling, A structural and morphological comparative study between chemically synthesized and photopolymerized poly (pyrrole), *J. Coat. Technol. Res.* **7**, 145 (2010).
15. S. Bilal and R. Holze, A correlation of electrochemical and spectroelectrochemical properties of poly (o-toluidine), *Electrochim. Acta*, **54**, 4851(2009).
16. M. V. Kulkarni and A. K. Viswanath, Comparative studies of chemically synthesized polyaniline and poly (o-toluidine) doped with p-toluene sulphonic acid, *Europ. Polym. Jour.*, **40**, 379 (2004).
17. M. Babazadeh, Aqueous dispersions of DBSA-doped polyaniline: One-pot preparation, characterization, and properties study, *J. Appl. Polym. Sci.*, **113**, 3980(2009).
18. M. V. Kulkarni, A. K. Viswanath, and P. Khanna, Synthesis and characterization of conducting polyaniline doped with polymeric acids, *J. Macromol. Sci., Part A: Pure Appl. Chem.*, **43**, 759(2006).
19. R. M. Issa, S. A. Azim, A. M. Khedr, and D. F. Draz, Synthesis, characterization, thermal, and antimicrobial studies of binuclear metal complexes of sulfa-guanidine Schiff bases, *J. Coord. Chem.*, **62**, 1859 (2009).



20. N. Puviarasan, V. Arjunan, and S. Mohan, FTIR and FT-Raman spectral investigations on 4-aminoquinoline and 5-aminoquinoline, *Turk.J. Chem.*, **28**, 53(2004).
21. K. Ravichandrika, P. Kiranmayi, and R. Ravikumar, Synthesis, characterization and antibacterial activity of ZnO nanoparticles, *Int. J. Pharm. Pharm. Sci.*, **4**, 0975(2012).
22. H. Kumar and R. Rani, Structural and optical characterization of ZnO nanoparticles synthesized by microemulsion route, *Int.Lett. Chem. Phys.Astron.*, **14**, 26(2013).
23. G. Paul, A. Bhaumik, A. Patra, and S. Bera, Enhanced photo-electric response of ZnO/polyaniline layer-by-layer self-assembled films, *Mater. Chem. Phys.*, **106**, 360(2007).
24. B. K. Sharma, N. Khare, S. Dhawan, and H. Gupta, Dielectric properties of nano ZnO-polyaniline composite in the microwave frequency range, *J.Alloys Comp.*, **477**,370 (2009).
25. P. Khiew, N. Huang, S. Radiman, and M. S. Ahmad, Synthesis and characterization of conducting polyaniline-coated cadmium sulphide nanocomposites in reverse microemulsion, *Mater. Lett.*, **58**, 516 (2004).
26. S. Kondawar, S. Bompilwar, V. Khati, S. Thakre, V. Tabhane, and D. Burghate, Characterizations of zinc oxide nanoparticles reinforced conducting polyaniline composites, *Arch. Appl. Sci. Res.*, **2**, 247(2010).
27. S. P. Sharma, M. Suryanarayana, A. K. Nigam, A. Chauhan, and L. Tomar, PANI/ZnO] composite: Catalyst for solvent-free selective oxidation of sulfides, *Catal. Commu.*, **10**,905 (2009).
28. S. Patil, S. Pawar, M. Chougule, B. Raut, P. Godse, S. Sen, et al., Structural, morphological, optical, and electrical properties of PANi-ZnO nanocomposites, *Int. J.Polym. Mater.*, **61**, 809 (2012).
29. H. Kunteppa, A. S. Roy, A. R. Koppalkar, and M. A. Prasad, Synthesis and morphological change in poly (ethylene oxide)-sodium chlorate based polymer electrolyte complex with polyaniline, *Physica B: Cond. Mat.*, **406**, 3997(2011).
30. S. Gul and S. Bilal, Synthesis and characterization of processable polyaniline salts, *J. Phys. Conf. Ser.*, 2013, 012002.
31. P. T. Patil, R. S. Anwane, and S. B. Kondawar, Development of electrospun polyaniline/ZnO composite nanofibers for LPG sensing, *Procedia Mater. Sci.* **10**, 195(2015).
32. R. Barde, Preparation, characterization and CO<sub>2</sub> gas sensitivity of Polyaniline doped with Sodium Superoxide (NaO<sub>2</sub>), *Mater. Res. Bull.*, **73**, 70 (2016).
33. S. P. Ansari and F. Mohammad, Studies on nanocomposites of polyaniline and zinc oxide nanoparticles with supporting matrix of polycarbonate, *ISRN Mater. Sci.*, 2012(2012).
34. S. Virji, J. Huang, R. B. Kaner, and B. H. Weiller, Polyaniline nanofiber gas sensors: examination of response mechanisms, *Nano Lett.*, **4**, 491(2004).
35. G. Khuspe, D. Bandgar, S. Sen, and V. Patil, Fussy nanofibrous network of polyaniline (PANi) for NH<sub>3</sub> detection, *Syn. Metals*, **162**, 1822(2012).
36. L. He, Y. Jia, F. Meng, M. Li, and J. Liu, Gas sensors for ammonia detection based on polyaniline-coated multi-wall carbon nanotubes, *Mater. Sci. Eng. B*, **163**, 76 (2009).